Real-Time Seismic Signal Enhancement Utilizing a Hybrid Rao–Blackwellized Particle Filter and Hidden Markov Model Filter

Erick Baziw, *Member, IEEE*

***Abstract*—This letter outlines a novel and robust algorithm for identifying seismic events within low signal-to-noise ratio (SNR) passive seismic data in real time. Since the event detection problem is a continuous, real-time process which has nonlinear mathematical representations, a Rao–Blackwellized particle filter (RBPF) is utilized. In this algorithm, a jump Markov linear Gaussian system (JMLGS) is defined where changes (i.e., jumps) in the state–space system and measurement equations are due to the occurrences and losses of events within the measurement noise. The RBPF obtains optimal estimates of the possible seismic events by individually weighting and subsequently summing a bank of Kalman filters (KFs). These KFs are specified and updated by samples drawn from a Markov chain distribution which defines the probability of the individual dynamical systems which compose the JMLGS. In addition, a hidden Markov model filter is utilized within the RBPF filter formulation so that real-time estimates of the phase of the seismic event can be obtained. The filter is demonstrated to provide up to an 80-fold improvement in the SNR when processing simulated seismic data with Gauss–Markov measurement noise.**

***Index Terms*—Acoustic signal detection, hidden Markov model (HMM), jump processes, Rao–Blackwellized particle filter (RBPF).**

I. Introduction

THERE is considerable interest in the engineering community in the real-time identification of "events" within time series data with low signal-to-noise ratio (SNR). This is especially true for acoustic emission analysis which is utilized for monitoring and inspecting the integrity and safety of many structures such as metal and concrete bridges, gas and oil pipelines, large storage tanks, and aerospace vehicles. A particular important application of acoustics emission analysis is within the field of passive seismology.

A passive seismic monitoring (PSM) system is designed to acquire and analyze, in real time, the acoustic signals collected by an array of appropriate seismic transducers. Seismic activity is often observed in the vicinity of underground excavations, deep open pits and quarries, around and below large reservoirs where fluids are being injected into, or removed from, permeable subsurface formations, and adjacent to the sites of large underground explosions [1].

Manuscript received February 23, 2005; revised May 24, 2005. This work was supported in part by the National Science and Engineering Research Council of Canada and the Consortium for the Development for Specialized Seismic Techniques (CDSST).

The author is with the Department of Earth and Ocean Sciences, University of British Columbia, Vancouver, BC Canada V6T 1Z4 (e-mail: staff@bcengineers.com).

Digital Object Identifier 10.1109/LGRS.2005.852711

Since the monitoring of seismic acoustic emissions is a continuous, real-time process which typically runs 24 h a day, seven days a week, it requires the incorporation of real-time passive seismic signal enhancement and event detection (PS-SEED) digital filters. These digital filters should also provide for time-variant, nonstationary, and nonlinear optimal estimation capabilities. To meet these requirements, a Bayesian recursive estimation (BRE) algorithm is implemented. The state–of-the-art BRE nonlinear estimation technique is the particle filter (PF) and its variants such as the Rao–Blackwellized particle filter (RBPF) [4]. The RBPF requires that the physical problem be formulated into linear and nonlinear components. The RBPF allows for a significant reduction in the number of particles required for estimating the posterior probability density function (pdf).

This PS-SEED filter outlined in this letter substantially builds upon previous original designs [2], [3]. In the PS-SEED algorithm, the seismic event is modeled as a frequency anomaly with time-variant phase which is embedded within Gauss–Markov measurement noise. As outlined in this letter, the major improvements to the PS-SEED algorithm consist of utilizing a RBPF which individually weights and subsequently sums a bank of linear Kalman filters (KFs) with jump Markov linear Gaussian system (JMLGS) characteristics. The JMLGS describes linear system and measurement equations which can change ("jump") with time (nonlinear component of JLMGS). In the PS-SEED filter, a hidden Markov model (HMM) filter is also applied, which allows for the determination of time-variant phase estimates if a seismic event is present.

II. Mathematical Background

A. Bayesian Recursive Estimation

Bayesian recursive estimation (BRE) is an optimal filtering technique which is based on state–space, time–domain formulations of physical problems. Application of this type of filter requires that the dynamics of the system and measurement model which relates the noisy measurements to the system state equations be describable in a mathematical representation and probabilistic form which, with initial conditions, uniquely define the system behavior.

The potentially nonlinear discrete stochastic equation describing the system dynamics is defined as follows:

$$\boldsymbol{x}_k = \boldsymbol{f}_{k-1}(\boldsymbol{x}_{k-1}, \boldsymbol{u}_{k-1}) \quad \leftrightarrow \quad p(\boldsymbol{x}_k | \boldsymbol{x}_{k-1}). \tag{1}$$

In (1), the vector $\boldsymbol{f}_k$ is a function of the state vector $\boldsymbol{x}_k$ and the process or system noise $\boldsymbol{u}_k$. It is assumed that (1) describes a Markov process of order one. The sampled potentially nonlinear measurement equation is given as

$$\boldsymbol{z}_k = \boldsymbol{h}_k(\boldsymbol{x}_k, \boldsymbol{v}_k) \quad \leftrightarrow \quad p(\boldsymbol{z}_k|\boldsymbol{x}_k). \tag{2}$$

In (2), $\boldsymbol{h}_k$ depends upon the index k, the state $\boldsymbol{x}_k$, and the measurement noise $\boldsymbol{v}_k$ at each sampling time. The probabilistic state–space formulation described by (1) and the requirement for updating the state vector estimate based upon the newly available measurements described by (2) are ideally suited for the Bayesian approach to optimal estimation.

In the Bayesian approach to optimal estimation, it is attempted to construct the posterior estimate of the state given all available measurements [4]. In general terms, it is desired to obtain estimates of the discretized system equation states $\boldsymbol{x}_k$ based on all available measurements up to time k (denoted as $\boldsymbol{z}_{1:k}$) by constructing the posterior $p(\boldsymbol{x}_k|\boldsymbol{z}_{1:k})$. The posterior pdf allows one to calculate the conditional mean estimate of the state ($E[\boldsymbol{x}_k|\boldsymbol{z}_{1:k}]$).

BRE is a two-step process consisting of prediction and update [4]. In the prediction step, the system equation defined by (1) is used to obtain the prior pdf of the state at time k via the Chapman–Kolmogorov equation, which is given as

$$p(\boldsymbol{x}_k|\boldsymbol{z}_{1:k-1}) = \int p(\boldsymbol{x}_k|\boldsymbol{x}_{k-1}) p(\boldsymbol{x}_{k-1}|\boldsymbol{z}_{1:k-1}) d\boldsymbol{x}_{k-1}. \tag{3}$$

The Chapman–Kolmogorov is derived based upon the transitional densities of a Markov sequence. The update step computes the posterior pdf from the predicted prior pdf and a newly available measurement. The posterior pdf is updated via Bayes' rule as follows:

$$p(\boldsymbol{x}_k|\boldsymbol{z}_{1:k}) = \frac{p(\boldsymbol{z}_k|\boldsymbol{x}_k) p(x_k|\boldsymbol{z}_{1:k-1})}{p(\boldsymbol{z}_k|\boldsymbol{z}_{1:k-1})}. \tag{4}$$

The recurrence equations defined by (3) and (4) form the basis for the optimal Bayesian solution. The BRE of the posterior density can be solved optimally (exact solution) when the state–space equations fit into a Kalman filter (KF) formulation or a HMM[4]. Otherwise, BRE requires a suboptimal numerical estimation approach when deriving the posterior pdf.

B. Kalman Filter and Jump Markov Linear Gaussian System

As previously stated, the standard set of KF equations can be implemented as an optimal solution to the BRE when certain conditions are met. These special conditions consist of the case where $\boldsymbol{u}_k$ and $\boldsymbol{v}_k$ are zero-mean independent Gaussian white noise processes, $\boldsymbol{f}_k$ is a linear function of the state vector and process noise, $\boldsymbol{h}_k$ is a linear function of the state vector and measurement noise, and the initial estimate of $\boldsymbol{x}_0$ has a Gaussian distribution [5].

Similar to the KF, a JMLGS is also defined as a linear Gaussian system, but in this case, the system and/or measurement equations ($\boldsymbol{f}_k$ and $\boldsymbol{h}_k$) evolve with time according to a finite state Markov chain [6]. Table I outlines the KF governing equations for a JMLGS [7]. The index i denoted in Table I facilitates the implementation of a bank of KFs when implementing an RBPF (subsequently outlined).

TABLE I
KF GOVERNING EQUATIONS FOR JMLGS

Description	Mathematical Representation	Eq.
Finite state Markov chain.	$y_k^i \sim P\left(y_k^i \mid y_{k-1}^j\right)$	5
System equation.	$\boldsymbol{x}_k^i = \boldsymbol{F}(y_k^i)\boldsymbol{x}_{k-1}^i + \boldsymbol{G}(y_k^i)\boldsymbol{u}_{k-1}^i$	6
Measurement equation.	$z_k^i = \boldsymbol{H}(y_k^i)\boldsymbol{x}_k^i + v_k^i$	7
State estimate extrapolation.	$\hat{\boldsymbol{x}}_{k\|k-1}^i = \boldsymbol{F}(y_k^i)\hat{\boldsymbol{x}}_{k-1\|k-1}^i$	8
Error covariance extrapolation.	$\boldsymbol{P}_{k\|k-1}^i = \boldsymbol{F}(y_k^i)\boldsymbol{P}_{k-1\|k-1}^i\boldsymbol{F}(y_k^i)^T + \boldsymbol{G}(y_k^i)\boldsymbol{Q}_{k-1\|k-1}^i\boldsymbol{G}(y_k^i)^T$	9
Measurement extrapolation.	$\hat{z}_k^i = \boldsymbol{H}(y_k^i)\hat{\boldsymbol{x}}_{k\|k-1}^i$	10
Innovation.	$\Delta_k^i = z_k^i - \hat{z}_k^i$	11
Variance of innovation.	$\boldsymbol{S}_k^i = \boldsymbol{H}(y_k^i)\boldsymbol{P}_{k\,k-1}^i\boldsymbol{H}(y_k^i)^T + \boldsymbol{R}_k^i$	12
Kalman gain matrix.	$\boldsymbol{K}_k^i = \boldsymbol{P}_{k\,k-1}^i\boldsymbol{H}(y_k^i)^T(\boldsymbol{S}_k^i)^{-1}$	13
State estimate update.	$\hat{\boldsymbol{x}}_{k\|k}^i = \boldsymbol{F}(y_k^i)\hat{\boldsymbol{x}}_{k\|k-1}^i + \boldsymbol{K}_k^i\Delta_k^i$	14
Error covariance update.	$\boldsymbol{P}_{k\backslash k}^i = \left[\boldsymbol{I} - \boldsymbol{K}_k^i\boldsymbol{H}(y_k^i)\right]\boldsymbol{P}_{k\|k-1}^i$	15

In (6) and (7) $\boldsymbol{v}_k$ and $\boldsymbol{u}_k$ are *i.i.d* Gaussian zero mean white noise processes with variances of $\boldsymbol{Q}_k$ and $\boldsymbol{R}_k$, respectively (i.e., $\boldsymbol{v}_k \sim N(0, \boldsymbol{R}_k)$ and $\boldsymbol{u}_k \sim N(0, \boldsymbol{Q}_k)$).

C. Hidden Markov Model Filter

The HMM filter (also termed a grid-based filter) has a discrete state–space representation and has a finite number of states. In the HMM filter the posterior pdf is represented by the delta function approximation as follows:

$$p(\boldsymbol{x}_{k-1}|\boldsymbol{z}_{1:k-1}) = \sum_{i=1}^{N_s} \boldsymbol{w}_{k-1\backslash k-1}^i \delta\left(\boldsymbol{x}_{k-1} - \boldsymbol{x}_{k-1}^i\right) \tag{16}$$

where $\boldsymbol{x}_{k-1}^i$ and $\boldsymbol{w}_{k-1|k-1}^i$, $i = 1, \ldots, N_s$, represent the fixed discrete states and associated conditional probabilities, respectively, at time index $k-1$, and N_s defines the number of particles utilized.

The governing equations for the HMM filter are derived by substituting (16) into the Chapman–Kolmogorov equation (3) and the posterior pdf update (4). This substitution results in the HMM prediction and update equations which are outlined in Table II [4].

D. Particle Filter and RBPF

1) Particle Filter: As stated previously, the recurrence equations defined by (3) and (4) form the basis for the optimal Bayesian solution and except for the KF and HMM exact solutions the BRE requires a suboptimal numerical estimation approach. To solve the BRE numerically, a new family of filters which rely upon sequential Monte Carlo methods have been

TABLE II
HMM FILTERING ALGORITHM

Step	Description	Mathematical Representation
1	Initialization (k=0) – initialize particle weights.	e.g., $w_k^i \sim 1/N_s$, $i = 1,\ldots,N_s$.
2	Prediction - predict the weights.	$w_{k\backslash k-1}^i = \sum_{j=1}^{N_s} w_{k-1\backslash k-1}^j p\left(x_k^i \mid x_{k-1}^j\right)$
3	Update - update the weights.	$w_{k\backslash k}^i = \frac{w_{k\backslash k-1}^i p\left(z_k \mid x_k^i\right)}{\sum_{j=1}^{N_s} w_{k\backslash k-1}^j p\left(z_k \mid x_k^j\right)}$
4	Obtain optimal minimum variance estimate of the state vector and corresponding error covariance.	$\hat{x}_k \approx \sum_{i=1}^{N_s} w_{k\backslash k}^i x_k^i$ & $P_{\hat{x}_k} \approx \sum_{i=1}^{N_s} w_{k\backslash k}^i (x_k^i - \hat{x}_k)(x_k^i - \hat{x}_k)^T$
5	Let k = k+1 & iterate to step 2.	

In the above equations it is required that the likelihood pdf $p(z_k \mid x_k^i)$ and the transitional probabilities $p(x_k^i \mid x_{k-1}^j)$ be known and specified.

TABLE III
PS-SEED FILTER FORMULATION

Step	Description	Mathematical Representation
1	Specify and initialize JMLGS system equations and N_s. Note: The measurement noise (v_k) variance R_k is set to $a1_k \times(\sigma_k)^2$ where $(\sigma_k)^2$ is the variance of the Gauss-Markov noise. This allows the filter to put more weight on the prior when the Gauss-Markov noise becomes more correlated from sample to sample.	System Dynamics $x_k = \begin{bmatrix} x1_k \\ x2_k \end{bmatrix} = \begin{bmatrix} a1_{k-1} & 0 \\ 0 & a2_{k-1} \end{bmatrix} \begin{bmatrix} x1_{k-1} \\ x2_{k-1} \end{bmatrix} + \begin{bmatrix} b1_{k-1} & 0 \\ 0 & b2_{k-1} \end{bmatrix} \begin{bmatrix} u1_{k-1} \\ u2_{k-1} \end{bmatrix}$ Measurement Equations Case 1 ($y1_k$ - ambient noise): $z_k^1 = x1_k + v_k$ Case 2 ($y2_k$ - ambient noise + event): $z_k^2 = x1_k + x2_k \sin(\omega k\Delta + \varphi_k) + v_k$
2	Initialize the prior and transitional pdf for the JMLGS.	$p(y_0^1)$, $p(y_0^2)$, & $p(y_k^j \mid y_{k-1}^j)$, $i,j=1,2$
3	Initialize the prior and transitional pdf for the fixed-grid phase.	$p(\varphi^j)$ & $p(\varphi^i \mid \varphi^j)$, $i,j = 1,\ldots,N_p$. N_p = *number of fixed-grid values.*
4	Draw samples for finite state Markov chain. Use HMM filter equations (Table II) to estimate φ_k^i if $y_k^i = y2_k$.	$y_k^i \sim P\left(y_k^i \mid y_{k-1}^j\right)$
5	Utilizing (8)-(12) outlined in Table I, propagate the system equations and calculate importance weights for particles.	$w_k^i = N(z_k \mid \hat{z}_k^i, S_k^i)$, , $i = 1,\ldots,N_s$.
6	Obtain sub-optimal estimate of the state vector.	$\hat{x}_k \approx \sum_{i=1}^{N_s} w_k^i x_k^i$
7	Sampling Importance Re-sampling (SIR). Re-sample if $\hat{N}_{eff} < N_T$	$\hat{N}_{eff} = \frac{N_s}{\sum_{i=1}^{N_s} (w_k^i)^2} < N_T$
8	Utilize (13)-(15) to update the bank of KFs	
9	Let k = k+1 & iterate to step 4.	

1) Parameters $a(1\text{-}2)_k$ and $b(1\text{-}2)_k$ define the Gauss-Markov processes and Δ is the sampling rate. Ambient noise parameters $a1_k$ and $b1_k$ are adaptively derived from the autocorrelation of the noise portion of the recorded time series. Parameters $a2_k$ and $b2_k$ are set by specifying 1/3 of the expected maximum possible variance of the amplitude of the seismic event and the corresponding time constant (i.e., correlation between samples) [3].

2) de Freitas [7] demonstrates that the importance weights, w_k^i, for y_k^i are given as $N(z_k; \hat{z}_k^i, S_k^i)$, where N denotes a Gaussian distribution.

made popular within the last decade. This family of new filters are most commonly referred to as particle filters.

Similar to the HMM filter, the PF represents the posterior pdf by the delta function approximation, but in this case a randomized grid is utilized for the estimation of the posterior pdf. For the PF, the weights in (16) are obtained using Bayesian importance sampling, and a typical PF algorithm is referred to as sequential importance sampling (SIS) [4]. An important component of the PF algorithm is to carry out a particle degeneracy check.

A common problem with the SIS approach is that after a few iterations, most particles have negligible weight (the weight is concentrated on a few particles only). This phenomenon is referred to as the degeneracy problem, and it is due to the fact that the variance of the importance weights increases over time. A simple statistics to monitor which gives an indication of the degeneracy is the effective sample size N_{eff}. An approximation to N_{eff} is given in Step 7 of Table III where N_s defines the number of particles utilized, and N_T is a user-specified threshold (e.g., $N_T = (0.6 \; to \; 0.8)N_s$). A small value of N_{eff} indicates severe degeneracy. The standard technique to counter the degeneracy problem is to resample the particles utilizing a Bayesian bootstrap technique [4] if the effective number of particles is less than N_T.

2) Rao–Blackwellized Particle Filter: The RBPF allows for the reduction in the number of required particles when implementing BRE on nonlinear systems. This is highly advantageous because even though there is a theoretical independence of accuracy from the particle dimension, practice has shown that the number of particles needs to be quite high for high-dimensional systems [8]. The RBPF can be utilized when the state–space model is described with both linear and nonlinear sets of equations.

In the RBPF implemented for PS-SEED a set of particles are generated by firstly computing the finite-state Markov chain distribution which is denoted as $P(y_k^i|y_{k-1}^i)$ in Table I. Second, based upon the samples drawn from $P(y_k^i|y_{k-1}^i)$ a bank of KFs (as outlined in Table I) is utilized to compute a set particles representing the possible seismic wavelet and ambient noise amplitudes and corresponding weights. The posterior pdf of the state vector is then calculated and subsequent suboptimal estimates obtained [7].

III. PS-SEED Filter Outline

The PS-SEED filter is based upon the standard short-term averaging/long-term averaging (STA/LTA) technique where an event is declared within the filtered time series when the STA/LTA ratio exceeds a predefined threshold [9]. In the PS-SEED digital filter, the seismic event is modeled as a frequency anomaly which is contained within measurement noise [2], [3]. The rationale for modeling the seismic event as a frequency anomaly is due to the difficulty in characterizing time-variant passive seismic source wavelets (e.g., ARMA model [10]) and for added robustness so that the filter can be applied in varied site conditions with minimal modifications.

A. State-Space Formulation

As outlined in [2] and [3], the measurement noise is modeled as a Gauss–Markov process with defining parameters of variance and time constant. This does not preclude any other types of ambient noise models, but it is required that the measurement noise be specified within a state–space formulation. The seismic event is modeled as an amplitude modulated cyclic waveform as follows (continuous form):

$$x_1(t) = x_2(t)\sin\left[\omega t + \varphi(t)\right] \tag{17}$$

where $x_1(t)$ is an approximation to the P-wave or S-wave seismic wavelet (the frequency anomaly), $x_2(t)$ is the seismic wavelet's amplitude response, ω is the dominant frequency of the wavelet, and $\varphi(t)$ is the corresponding phase.

In [2] and [3], state $x_2(t)$ was approximated as a random walk process, ω was assumed constant, and $\varphi(t)$ was derived in an ad hoc manner. To allow for greater flexibility, the PS-SEED models state $x_2(t)$ as a Gauss–Markov process similar to that outlined for the ambient noise model. More sophisticated amplitude models can be implemented such as the formulation of a Taylor series on the amplitude dynamics carried out to a third term. The third term (acceleration) is then modeled as a Gauss–Markov process. In the PS-SEED formulation outlined in this letter, it is again assumed that ω is constant (i.e., the investigator is looking for a dominant frequency which represents the P-wave or S-wave), while $\varphi(t)$ is derived by implementing a HMM filter.

B. PS-SEED RBPF and HMM Filter Implementation

In general terms, the PS-SEED obtains estimates of the possible seismic events by utilizing a RBPF which individually weights and subsequently sums a bank of KFs which describe the physics of the ambient noise and seismic event. These KFs are specified and updated by samples drawn from a Markov chain distribution which defines the probability of the individual dynamical systems which compose the JMLGS [7]. In addition, a HMM filter is applied which determines optimal $\varphi(t)$ values if a seismic event is present. Table III outlines the PS-SEED filter formulation.

IV. Simulation Results

This section outlines the performance of the PS-SEED for the specific case of a periodic exponentially decaying source wavelet embedded within Gauss–Markov noise with widely varying time constants and high variances. The seismic event is modeled with defining parameters of initial amplitude, damping factor, and dominant angular frequency ($\omega = 2\pi \mathrm{f}$) [2]. The simulated seismic event had a frequency of 200 Hz (selected to reflect typical P-waves recorded by PSM systems within sedimentary deposits [2], [3]), initial amplitude of 160 mm/s^2, and damping factor of 79/s specified. The sampling rate was set at 0.05 ms, and a total sampling time of 300 ms was specified. Fig. 1(a) illustrates the source wavelet generated with the previously specified parameters.

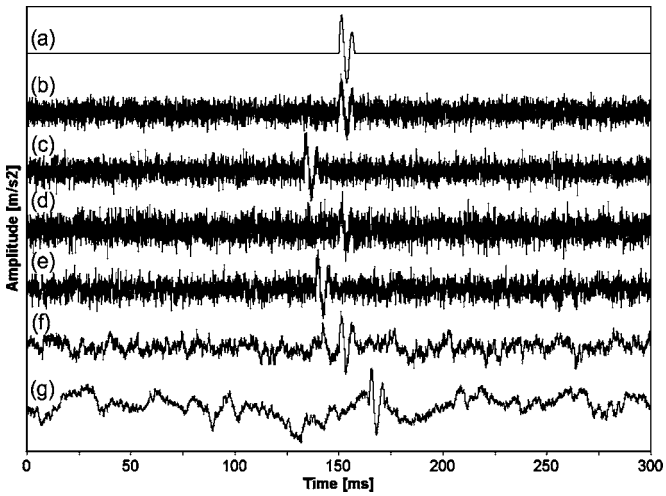

Fig. 1. Source wavelet embedded with varying types of Gauss–Markov background noise.

Fig. 1(b)–(g) shows the simulated source wavelet with additive Gauss–Markov noise with variances and time constants specified as (1000 mm^2/s^4, 0.0001 ms), (1000 mm^2/s^4, 0.0001 ms), (4000 mm^2/s^4, 0.0001 ms), (1000 mm^2/s^4, 0.1 ms), (1000 mm^2/s^4, 1.0 ms), and (2000 mm^2/s^4, 10 ms), respectively. The source wavelet had an arrival time of 150 ms [$\varphi = 0^\circ$ in (17)] specified for the simulated traces illustrated in Fig. 1(b), (d), and (f). In Fig. 1(c), (e), and (g), the source wavelet had arrival times of 133 ms ($\varphi = 140^\circ$), 138.7 ms ($\varphi = 90^\circ$), and 164.4 ms ($\varphi = 45^\circ$) specified, respectively. In Fig. 1, the units of the amplitudes of the time series data are not displayed in order to reduce clutter and due to the fact that the STA/LTA event detection technique is only dependent upon relative amplitudes.

The initialization of the JMLGS system equations (Case 1 and 2 of Step 1 in Table III) was carried out similarly to that outlined in [2]. The initialization of the finite-state Markov chain probabilities are based upon the likelihood of an event occurring and the transitional probability of moving from a nonevent to an event. The pdfs and transitional pdfs were set to $p(y_0^1) = 0.9$, $p(y_0^2) = 0.1$, $p(y_k^1|y_{k-1}^1) = 0.8$, $p(y_k^1|y_{k-1}^2) = 0.8$, $p(y_k^2|y_{k-1}^2) = 0.2$, and $p(y_k^2|y_{k-1}^1) = 0.2$, respectively, for the simulations presented here. In general terms, the probability of an event is about 20%. The initialization of the pdf of the time-variant phase was set to the uniform distribution, while the fixed-grid transitional pdf $p(\varphi_k^i|\varphi_{k-1}^i)$ is set quite high (e.g., 0.996), and the remaining values are set to have a uniform distribution. There were 90 (N_p) phases specified to reflect the possible phase shifts of 0° to 180° in

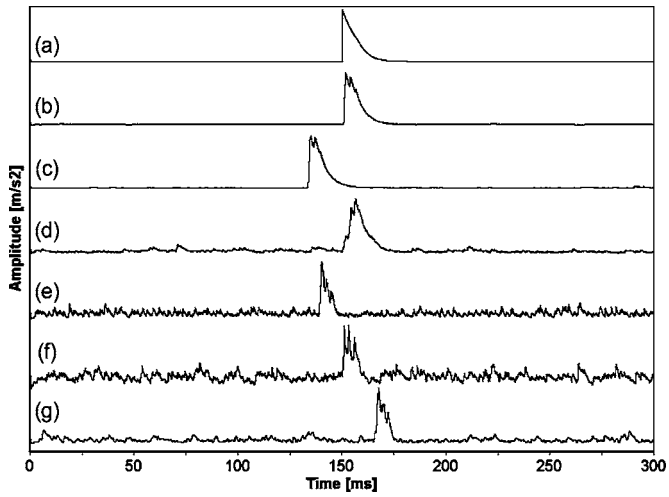

Fig. 2. PS-SEED output results for estimating state $\hat{x}2_k$ after processing the data shown in Fig. 1.

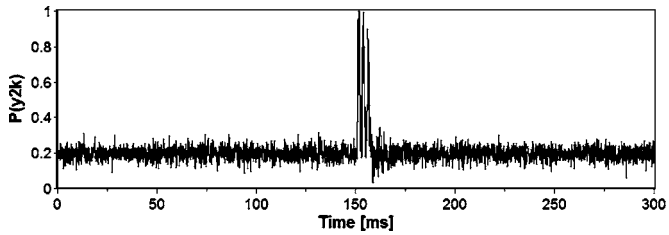

Fig. 3. Estimated probability of an event $P(y2_k|z_{1:k})$ for the test case shown in Fig. 1(b). The first maximum is selected as it corresponds to the first break [3] of the source wavelet.

2° increments. The number of particles (N_s) specified for the PS-SEED filter was 100. The degeneracy threshold parameter N_T was set to 0.8 N_s.

The PS-SEED filter was implemented on the simulated data illustrated in Fig. 1 with the output for state $\hat{x}2_k$ (seismic amplitude) illustrated in Fig. 2(b)–(g). Fig. 2(a) shows the true amplitude of the simulated wavelets. As is illustrated in Fig. 2(b)–(g), there is a significant real-time SNR improvement after implementation of the PS-SEED algorithm. In these test cases, the SNR is defined as the ratio of the average maximum amplitude of the signal to the maximum average amplitude of the noise. The PS-SEED was able to increase the SNR by approximately 80-fold, 80-fold, 30-fold, 10-fold, 9-fold, and 11-fold for the Gauss–Markov additive noise illustrated in Figs. 1(b)–(g), respectively. The lower SNR is due to the noise characteristics more closely matching those of the source wavelet making real-time noise/signal separation more difficult. The HMM filter portion of the PS-SEED algorithm also did a good job of estimating the phase shifts for the source wavelets illustrated in Fig. 1 as indicated by the responses shown in Fig. 2. Fig. 3 illustrates the estimated probability of an event $(P(y2_k|z_{1:k}))$ for the test case shown in Fig. 1(b). As expected, the probability of an event increases along with the seismic amplitude estimate illustrated in Fig. 2(b).

V. Conclusion

This letter has outlined a BRE algorithm which utilizes a hybrid RBPF and a HMM filter for the purpose of identifying events during passive seismic monitoring. The event detection algorithm builds upon previous designs where the major improvements consist of modeling the problem as a JMLGS and the implementation of a HMM filter for quantifying the phase of the seismic events. Simulation results were presented where source wavelets with additive Gauss–Markov background noise were analyzed and results evaluated in terms of the improvement in signal-to-noise ratio. There is up to an 80-fold improvement in signal-to-noise ratio after implementation of the PS-SEED.

Although the described filter has been utilized for automating the identification of seismic events during passive seismic investigations, the filter is easily applied to many other acoustic emission problems requiring real-time event detection. It is also the intention of the author to update the PS-SEED filter so that it not only gives real-time phase estimates but also quantifies the frequency content of the seismic events.

Acknowledgment

The author would like to thank T. Ulrych for his support and helpful suggestions.

References

[1] S. J. Gibowicz and A. Kijko, *An Introduction to Mining Seismology*. San Diego, CA: Academic, 1994, ch. 1.
[2] E. Baziw and I. Weir-Jones, "Application of Kalman filtering techniques for microseismic event detection," *Pure Appl. Geophys.*, vol. 159, pp. 449–473, Jan. 2002.
[3] E. Baziw, B. Nedilko, and I. Weir-Jones, "Microseismic event detection Kalman filter: Derivation of the noise covariance matrix and automated first break determination for accurate source location estimation," *Pure Appl. Geophys.*, vol. 161, pp. 303–329, Feb. 2004.
[4] M. S. Arulampalam, S. Maskell, and T. Clapp, "A tutorial on particle filters for online nonlinear/non-Gaussian Bayesian tracking," *IEEE Trans. Signal Process.*, vol. 50, no. 2, pp. 174–188, Feb. 2002.
[5] A. Gelb, *Applied Optimal Estimation*, 4th ed. Cambridge, MA: MIT Press, 1974.
[6] A. Doucet, N. J. Gordon, and V. Krishnamurthy, "Particle filters for state estimation of jump Markov linear systems," *IEEE Trans. Signal Process.*, vol. 49, no. 3, pp. 613–624, Mar. 2001.
[7] N. de Freitas, "Rao–Blackwellised particle filtering for fault diagnosis," in *Proc. IEEE Aerospace Conf.*, vol. 4, 2002, pp. 1767–1772.
[8] F. Gustafsson, F. Gunnarsson, N. Bergman, U. Forssell, J. Jansson, R. Karlsson, and P. Nordlund, "Particle filters for positioning, navigation, and tracking," *IEEE Trans. Signal Process.*, vol. 50, no. 2, pp. 425–435, Feb. 2002.
[9] R. V. Allen, "Automatic earthquake recognition and timing from single traces," *Bull. Seismol. Soc. Amer.*, vol. 68, pp. 1521–1532, 1978.
[10] E. Baziw, "State-space seismic cone minimum variance deconvolution," in *Proc. 2nd Int. Conf. Geotechnical Site Characterization (ISC-2)*, Porto, Portugal, Sep. 19–22, 2004, pp. 835–842.